Sequential Gas-Solid Reactions

A model is developed describing consecutive gas-solid reactions occurring in porous media. The model calls for independently measurable parameters and predicts two maxima in the reaction rate at intermediate conversions. The low temperature (350°C) reduction of hematite to iron in a hydrogen-nitrogen atmosphere was used to test the model. The experimental data confirmed the expected rate maxima. The conversion predictions are very close to the data for conversions below 30%, but are systematically somewhat lower than the experimental values for higher levels of conversion. An explanation for the discrepancy is offered in terms of the description of the pore structure.

Arthur J. Fortini
Daniel D. Perlmutter
Department of Chemical Engineering
University of Pennsylvania
Philadelphia, PA 19104

The problem of modeling gas-solid reactions that occur in sequence, where the porous solid product of the first reaction becomes the reactant for the second, is discussed in this paper. A model is developed that allows for two maxima in the reaction rate at intermediate conversions. To test the model, new experimental results are reported on two chemical reactions that were previously studied only individually (Fortini and Perlmutter, 1989). In these new experiments the reactions were intentionally sequenced, rather than run one at a time.

Model Development

Consider the two-step reaction sequence

$$aA(s) + pP(g) \rightarrow bB(s) + qQ(g) \tag{1}$$

$$bB(s) + rR(g) \rightarrow cC(s) + sS(g) \tag{2}$$

where A, B, and C are porous solids. The first reaction takes place on the surface of all the pores initially present in the sample. In its wake, it leaves behind a shell of B which can have its own micropore structure. The second reaction occurs when the B that has been formed begins to form C. It is convenient at this point to differentiate between the Level-1 pores, those present in the starting material before any reactions take place and the Level-2 pores, those formed by the first reaction. If a completely nonporous sample of A is reacted to form B, all the pores present in the B phase will be Level-2 pores. Otherwise, both Level-1 and Level-2 pores will coexist.

Pore structure in levels

If it is assumed that in the absence of sintering the pore structure of the Level-1 pores remains unchanged during the formation of the Level-2 pores, then

$$\epsilon_{12} = \epsilon_1 + \epsilon_2 \tag{3}$$

$$S_{12} = S_1 + S_2 \tag{4}$$

and by dividing:

$$\frac{S_{12}}{1 - \epsilon_{12}} = \frac{S_1}{1 - \epsilon_1 - \epsilon_2} + \frac{S_2}{1 - \epsilon_1 - \epsilon_2} \tag{5}$$

Since each $\epsilon > 0$:

$$\frac{S_{12}}{1 - \epsilon_{12}} > \frac{S_1}{1 - \epsilon_1} + \frac{S_2}{1 - \epsilon_2} \tag{6}$$

Using the same arguments, it is also true that if

$$L_{12} = L_1 + L_2 \tag{7}$$

then

$$\frac{L_{12}}{1 - \epsilon_{12}} > \frac{L_1}{1 - \epsilon_1} + \frac{L_2}{1 - \epsilon_2} \tag{8}$$

Step 1: A → B

As the first reaction progresses, the A/B interface moves radially outward from the surface of the Level-1 pores. Eventually these interfaces intersect, resulting in a decrease in reaction surface area and hence a decrease in reaction rate. For reactions under kinetic control, this situation can be quantitatively described by the random pore model of Bhatia and Perlmutter

(1980, 1981, 1983). In dimensional terms, the governing equations are

$$X_1 = 1 - \exp\left[-R_1^1 t - \frac{\Psi_1 (R_1^1)^2}{4} t^2\right] \tag{9}$$

and

$$\frac{dX_1}{dt} = R_1^1(1 - X_1)\sqrt{1 - \Psi_1 \ln(1 - X_1)} \tag{10}$$

where R_1^1 is the reaction rate given by

$$R_1^1 = \frac{\mathcal{R}_1 S_1}{1 - \epsilon_1} \tag{11}$$

and Ψ is a pore structure parameter given by

$$\Psi_i = \frac{4\pi L_i (1 - \epsilon_i)}{S_i^2} \tag{12}$$

The superscript on R refers to the level of pore structure where the reaction is taking place, and the subscript denotes which reaction is occurring.

Step 2: B → C

To describe the second reaction it is necessary to take a closer look at the pore structure. As the first reaction takes place on the surface of the Level-1 pores and the reaction interface moves radially outward, the second reaction takes place on all accessible surfaces of the B phase. This includes the surfaces of the Level-2 pores as they are being formed, as well as the surfaces of the Level-1 pores.

Figure 1 shows schematically the region surrounding a Level-1 pore, where only a single Level-2 pore is shown for clarity. Annular regions where both reactions have gone to completion are adjacent to the Level-1 and Level-2 pores shown by the darkened areas in the figure. Because there are two well-defined interfaces moving radially outward from the Level-1 pore, it is possible to define three zones of reaction, as shown in Figure 2. The conversion of the second reaction will be the sum of the volume-weighted contributions from each of the three zones.

In zone I the conversion of the second reaction is unity, and the volume fraction V_1 is the volume swept by the Zone-I/Zone-II interface divided by the total volume that would be swept if the reaction were allowed to go to completion. It can also be thought of as the conversion of the second reaction if there were no contribution from Level-2 pores. Hence

$$V_1(t) = 1 - \exp\left[-R_2^1 t - \frac{\Psi_1 (R_2^1)^2}{4} t^2\right] \tag{13}$$

The volume fraction of Zone II is given by $(V_2 - V_1)$, where

$$V_2(t) = 1 - \exp\left[-R_1^1 t - \frac{\Psi_1 (R_1^1)^2}{4} t^2\right] \tag{14}$$

In Zone III, the conversion of the second reaction (as well as of the first reaction) is zero, and this zone does not contribute to the overall conversion of the second reaction.

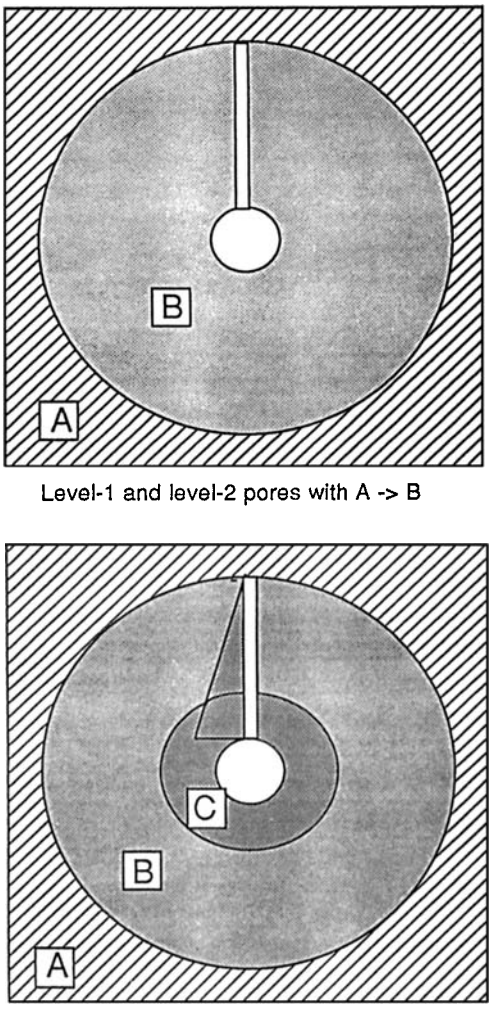

Figure 1. Product growth around Level-1 and Level-2 pores.

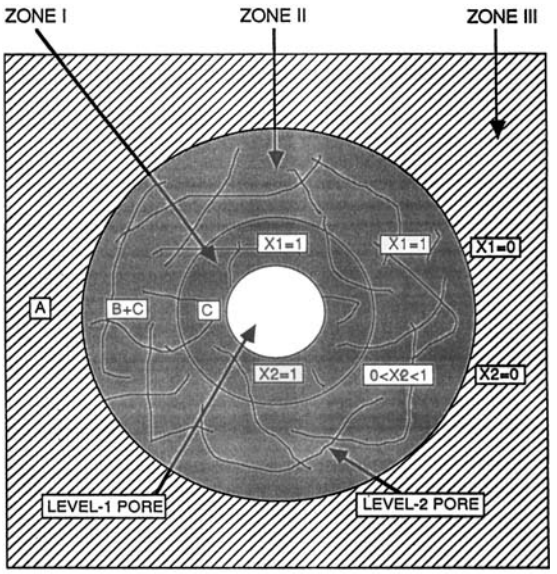

Figure 2. Three zones of reaction surrounding Level-1 pore.

To compute the average local conversion in Zone II, it is necessary to work with the reaction occurring on the surface of the Level-2 pores. The local conversion behavior of the second reaction in this zone is given by

$$X_2^*(T) = 1 - \exp\left[-R_2^2 T - \frac{\Psi_2 (R_2^2)^2}{4} T^2\right] \qquad (15)$$

where T is the duration of time that a particular volume element of B has been reacting to form C. By using as a weighting function the volume of B that has been reacting for time T, integration of the local conversion over values of T that can be achieved in Zone II gives for the overall conversion of the second reaction:

$$X_2(t) = V_1(t) + \int_0^{\alpha t} \frac{dX_1}{dt} (t - T)\, X_2^*(T)\, dt \qquad (16)$$

where $\alpha = (\mathcal{R}_1 + \mathcal{R}_2)/\mathcal{R}_1$. The lower limit of T is zero since any element of B that has just been formed by the first reaction (at the interface between Zones II and III) will have had no time to react to form C. The upper limit is the total time of reaction for an element of B in Zone II at the Zone I/Zone II interface.

When the overall rates of the two reactions are comparable or when the first reaction is of particular interest, Eq. 9 and 16 can be scaled by the rate of the first reaction to give the dimensionless equations

$$X_1(\tau) = 1 - \exp\left[-\tau - \frac{\Psi_1}{4}\tau^2\right] \qquad (17)$$

and

$$X_2(\tau) = V_1(\tau) + \int_0^{\alpha\tau} \frac{dX_1}{d\tau} (\tau - \theta)\, X_2^*(\theta)\, d\theta \qquad (18)$$

where $\tau = R_1^1 t$, $\theta = R_1^1 T$, and

$$V_1(\tau) = 1 - \exp\left[-(1-\alpha)\tau - \frac{\Psi_1 (1-\alpha)^2}{4}\tau^2\right] \qquad (19)$$

$$\frac{dX_1}{d\tau}(\tau - \theta) = \left[1 + \frac{\Psi_1}{2}(\tau - \theta)\right] \exp\left[-(\tau - \theta) - \frac{\Psi_1}{4}(\tau - \theta)^2\right] \qquad (20)$$

$$X_2^*(\theta) = 1 - \exp\left[-\left(\frac{R_2^2}{R_1^1}\theta\right) - \frac{\Psi_2}{4}\left(\frac{R_2^2}{R_1^1}\theta\right)^2\right] \qquad (21)$$

The net conversion of the overall reaction sequence may be written as

$$X_{\text{tot}}(\tau) = yX_1(\tau) + (1 - y)X_2(\tau) \qquad (22)$$

where y is the total fractional mass change associated with the first reaction.

Numerical results

Figures 3 and 4 show computed rates of the overall reaction for several values of Ψ_1 and Ψ_2, respectively, demonstrating the existence of two local maxima with respect to conversion. As was the case for the single-step random pore model (Bhatia and Perlmutter, 1980, 1981, 1983), the rate increases with increase in the value of Ψ_1. Figures 5 and 6 show the conversion predictions for several values of the groups R_2^2/R_1^1 and α, respectively. It may be noted that the second maximum in rate decreases as R_2^2/R_1^1 is increased and vanishes entirely as α is decreased sufficiently. The overall rate of reaction increases with increase in y.

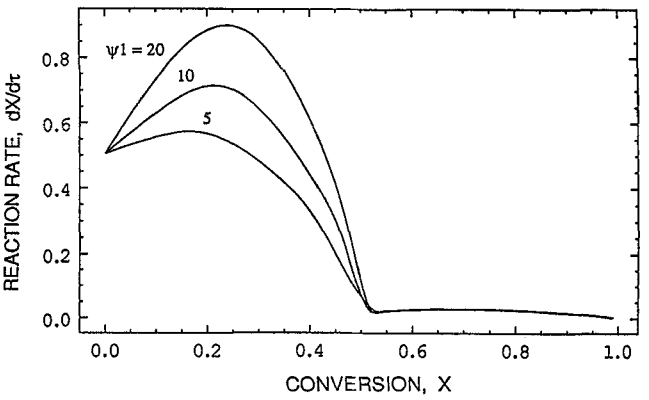

Figure 3. Reaction rate v. conversion for several values of Ψ_1.
$\Psi_2 = 75$, $R_2^2/R_1^1 = 0.015$, $\alpha = 0.99$, $y = 0.5$.

Experimental Results and Discussion

To test the model, the sequential reactions

$$3\,Fe_2O_3 + H_2 \rightarrow 2\,Fe_3O_4 + H_2O \qquad (23)$$

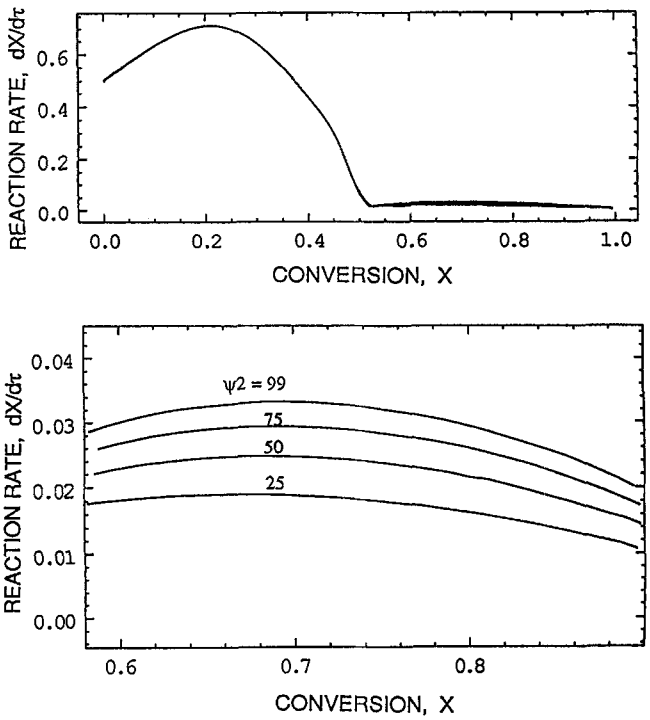

Figure 4. Reaction rate v. conversion for several values of Ψ_2.
$\Psi_1 = 5$, $R_2^2/R_1^1 = 0.015$, $\alpha = 0.99$, $y = 0.5$.

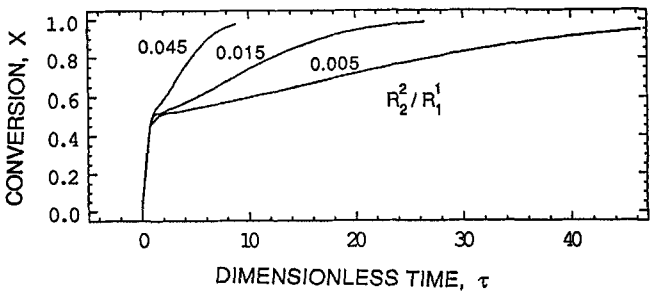

Figure 5. Conversion v. dimensionless time for several values of R_2^2/R_1^1.
$\Psi_1 = 5, \Psi_2 = 75, \alpha = 0.99, y = 0.5$.

and

$$Fe_3O_4 + 4\,H_2 \rightarrow 3\,Fe + 4\,H_2O \qquad (24)$$

were studied in the temperature range of 290 to 540°C in atmospheres containing hydrogen and water vapor as reactants and nitrogen as a diluent. The conditions were chosen to insure that iron would be the final product, rather than magnetite.

Experimental results on the direct conversion of hematite (through magnetite) to iron are reported in Figure 7, superimposed on the predicted curve computed from the model equation (Eq. 22). The experimental reproducibility may be assessed by noting that every second point is from a duplicate run. The calculations called for specification of the rates R_1^1, R_2^1, and R_2^2, as well as the pore structure parameters Ψ_1 and Ψ_2. These were obtained from the prior evaluations done on the individual reaction steps and reported earlier (Fortini and Perlmutter, 1989).

The results in Figure 7 show agreement between the model and data in predicting the two rate maxima. The numerical details agree to within 4% for conversions of less than 30%, but show a small systematic deviation of less than 0.1 conversion units at higher conversions. The expanded scale used for Figure 8 emphasizes the excellent agreement at low conversions.

To understand why the model predictions might be low in a specific case, it is instructive to examine the limiting case where the first reaction ($A \rightarrow B$) occurs instantly at $t = 0$, such that $X_1(\theta) = \delta(\theta)$ and Eq. 16 reduces to

$$X_2(t) = V_1(t) + [1 - V_1(t)]\, X_2^*(t) \qquad (25)$$

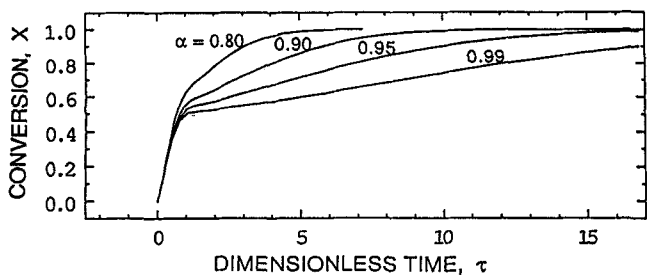

Figure 6. Conversion v. dimensionless time for several values of α.
$\Psi_1 = 5, \Psi_2 = 75, R_2^2/R_1^1 = 0.015, y = 0.5$

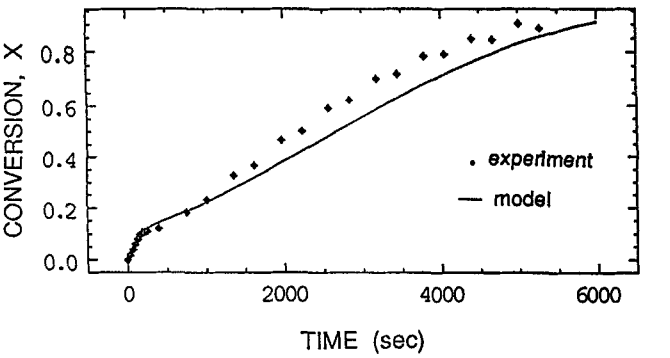

Figure 7. Conversion v. time behavior for reduction of hematite to iron.
$P_H = 0.45, P_W = 0$.

This is equivalent to a sample of B reacting with pore structure parameter Ψ_{12}, where

$$\Psi_{12} = \frac{4\pi\,(L_1 + L_2)\,(1 - \epsilon_1 - \epsilon_2)}{(S_1 + S_2)^2} \qquad (26)$$

Hence

$$X_2(R_2^{12}, t) = V_1(R_2^1, t) + [1 - V_1(R_2^1, t)]\, X_2(R_2^2, t) \qquad (27)$$

where, as before, the superscripts refer to the pore structure upon which the reaction is taking place. Substituting Eq. 13 and 15 yields:

$$R_2^{12}t + \frac{\Psi_{12}\,(R_2^{12})^2}{4}t^2 = R_2^1 t + \frac{\Psi_1\,(R_2^1)^2}{4}t^2 + R_2^2 t + \frac{\Psi_2\,(R_2^2)^2}{4}t^2 \qquad (28)$$

and equating like powers of t generates the two conditions

$$R_2^{12} = R_2^1 + R_2^2 \qquad (29)$$

and

$$(R_2^{12})^2\,\Psi_{12} = (R_2^1)^2\,\Psi_1 + (R_2^2)^2\,\Psi_2 \qquad (30)$$

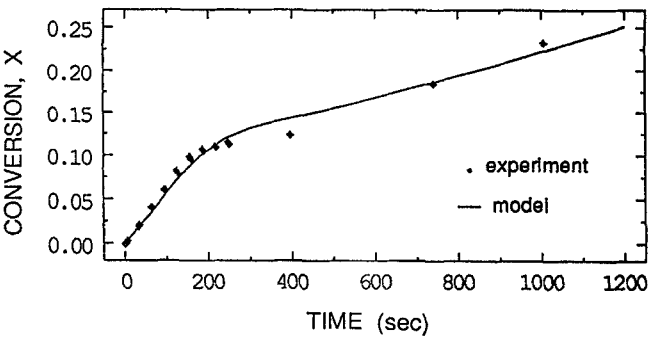

Figure 8. Conversion v. time behavior for reduction of hematite to iron.
$P_H = 0.45, P_W = 0$.

These conditions will be satisfied if:

$$\frac{S_{12}}{1-\epsilon_{12}} = \frac{S_1}{1-\epsilon_1} + \frac{S_2}{1-\epsilon_2} \tag{31}$$

and

$$\frac{L_{12}}{1-\epsilon_{12}} = \frac{L_1}{1-\epsilon_1} + \frac{L_2}{1-\epsilon_2} \tag{32}$$

Comparing this result with inequalities 6 and 8 shows that the model has an approximation built in, the extent of which depends on the degree to which the actual pore structure deviates from Eq. 31 and 32. For the case at hand:

$$\frac{S_{12}}{1-\epsilon_{12}} = 1.20 \times 10^6 \text{cm}^{-1} \tag{33}$$

$$\frac{S_1}{1-\epsilon_1} + \frac{S_2}{1-\epsilon_2} = 1.14 \times 10^6 \text{cm}^{-1} \tag{34}$$

a discrepancy of 5%, and

$$\frac{L_{12}}{1-\epsilon_{12}} = 2.61 \times 10^{12} \text{cm}^{-2} \tag{35}$$

$$\frac{L_1}{1-\epsilon_1} + \frac{L_2}{1-\epsilon_2} = 2.12 \times 10^{12} \text{cm}^{-2} \tag{36}$$

a discrepancy of 21%. Since these deviations are of significant magnitude, it is to be expected that the data shown in Figure 7 are somewhat higher than the model prediction.

Notation

L_i = total pore length of Level-i pores at $t = 0$, cm/cm^3
P_H = hydrogen partial pressure, atm
P_W = water vapor partial pressure, atm
R_i^j = rate of reaction i occurring on Level-j pores, 1/s
$\mathcal{R}_i$ = rate of reaction i, cm/s
S_i = total pore surface area of Level-i pores at $t = 0$, cm^2/cm^3
t = time
T = duration of $B \rightarrow C$ reaction
V_i = volume fraction of solid swept by reaction interface i
X_i = fractional conversion of reaction i
X_2^* = local fractional conversion of reaction 2
y = mass change of sample due to the first reaction/total possible mass change from all reactions

Greek letters

α = reaction rate ratio $= 1 + (\mathcal{R}_2/\mathcal{R}_1)$
ϵ_i = porosity of Level-i pores at $t = 0$
τ = dimensionless time $= R_1^1 t$
θ = dimensionless time $= R_1^1 T$
Ψ_i = pore structure parameter of Level-i pores defined in Eq. 12

Literature Cited

Bhatia, S. K., and D. D. Perlmutter, "A Random Pore Model for Fluid-Solid Reactions: I. Isothermal, Kinetic Control," *AIChE J.*, **26**, 379 (1980).

———, "A Random Pore Model for Fluid-Solid Reactions: II. Diffusion and Transport Effects," *AIChE J.*, **27**, 247 (1981).

———, "Unified Treatment of Structural Effects in Fluid-Solid Reaction," *AIChE J.*, **29**, 281 (1983).

Fortini, A. J., and D. D. Perlmutter, "Porosity Effects in Hydrogen Reduction of Iron Oxides," *AIChE J.*, **35**, 1245 (1988).

Manuscript received Feb. 15, 1989, and revision received Sept. 25, 1989.